A two pathway model for N2O emissions by ammonium oxidizing bacteria supported by the NO/N2O variation

Mathieu Pocquet, Z Wu, Isabelle Queinnec, M Spérandio

A two pathway model for N_2O emissions by ammonium oxidizing bacteria supported by the NO/N_2O variation

M. Pocquet[1,2,3,4], Z. Wu[1,2,3], I. Queinnec [4], M. Spérandio[1,2,3*]

[1] Université de Toulouse; INSA, UPS, LISBP, 135 Avenue de Rangueil, F-31077 Toulouse, France

[2] INRA, UMR792 Ingénierie des Systèmes Biologiques et des Procédés, F-31400 Toulouse, France

[3] CNRS, UMR5504, F-31400 Toulouse, France.

[4] CNRS; LAAS; 7 avenue du colonel Roche, F-31077 Toulouse Cedex 4, France

corresponding author: sperandio@insa-toulouse.fr

Abstract

In this work, a new model for nitritation combining two N_2O emission pathways was confronted with both NO and N_2O measurements during nitrification. The model was calibrated with batch experiments and validated with long-term data collected in a sequencing batch reactor (SBR). A good prediction of the evolution of N_2O emissions for a varying level of nitrite was demonstrated. The NO/N_2O ratio was shown to vary during nitritation depending on the nitrite level. None of the models based on a single pathway could describe this variation of the NO/N_2O ratio. In contrast, the 2 pathway model was capable of describing the trends observed for the NO/N_2O ratio and gave better predictions of N_2O emission factors. The model confirmed that the decrease of the NO/N_2O ratio can be explained by an increase of the ND pathway to the detriment of the NN pathway. The ND pathway was systematically the predominant pathway during nitritation. The combined effect

of nitrite (or free nitrous acid) and dissolved oxygen (DO) on the contribution of each pathway was in agreement with practical observations and the literature.

Keywords: Modelling, Nitric oxide, Nitrous oxide, Production pathways, Nitritation, Ammonia oxidizing bacteria.

1 INTRODUCTION

Both nitrous oxide (N_2O) and nitric oxide (NO) can be produced during nitrification and denitrification in wastewater treatment plants (Schreiber et al., 2012; Kampschreur et al., 2009). Nitrous oxide (N_2O) is a key greenhouse gas (GHG) with a global warming potential 300 times stronger than carbon dioxide and a long lifetime in the atmosphere (121 years). Nitric oxide (NO) is toxic to micro-organisms (Zumft, 1993) and both NO and N_2O are involved in ozone layer depletion (Crutzen, 1979). N_2O emissions from wastewater treatment are reported to have constituted 3.56% of the total anthropogenic N_2O emissions in 2010 (Fischedick et al., 2014) and have increased by almost 25% in 20 years. Recent measurement campaigns on real WWTPs have shown that the N_2O emission factor (N_2O-EF) can vary from 0.17% to 2.8%, (Daelman et al., 2013; Ye et al., 2014) and the gas can account for up to 78% of the total climate footprint of the plant (Daelman et al., 2013). Nitrification (by ammonium oxidizing bacteria) has been identified as a major contributor to N_2O production in wastewater treatment (Kampschreur et al., 2009, Daelman et al., 2013).

Mathematical dynamic modelling of N_2O emission is of great importance in the search for mitigation strategies based on optimal design and control. Among the different possible mechanisms for N_2O production by AOB, two pathways are now considered to be the major

processes responsible for the emissions during nitrification (Chandran et al., 2011; Wunderlin et al., 2012). The first major pathway corresponds to the autotrophic denitrification of nitrite (noted "ND") (Kim et al., 2010), i.e. the reduction of nitrite to NO by the NirK enzyme, followed by the reduction of NO to N_2O by the Nor enzyme. The second pathway (noted "NN") is incomplete hydroxylamine oxidation by the HAO enzyme (Chandran et al., 2011; Law et al., 2012; Stein, 2011), resulting in the accumulation of NO, which is then reduced to N_2O by the Nor enzyme.

At least four different models based on single pathways have been proposed and confronted with different lab-scale or full-scale N_2O measurements (Ni et al., 2013a; Spérandio et al., 2015) leading to satisfactory descriptions in various cases. However the conclusions of these calibration exercises, with either batch results (Ni et al., 2013a) or continuous long-term data (Spérandio et al., 2015), were that it was not possible to find a single model structure based on a single pathway that could describe all the data published in the literature. The main assumption formulated was that both NN and ND pathways can occur at the same time and the contribution of each of them would depend on the operating conditions. The regulation between the two main N_2O production pathways of AOB has been partially elucidated by recent works based on isotope signature measurements (Peng et al., 2014; Wunderlin et al., 2013). These works show that the nitrite (or the free nitrous acid) and the dissolved oxygen both play key roles in this regulation. During ammonium oxidation in batch experiments, the ND pathway is dominant and increases with time. The contribution of ND has been shown to increase as DO decreases under 1 mgO_2/L whereas the contribution of NN pathway increases with the DO (Peng et al., 2014). The contribution of the ND pathway also increases with nitrite accumulation at low DO level (Wunderlin et al., 2013). However it has also been supposed that the ND pathway is inhibited at very high nitrite concentrations, from 50 to 1000

$mgN.L^{-1}$ (Law et al., 2013). Finally a comparative calibration work indicated that models based on the NN pathway matched the data from systems with relatively low nitrite accumulation (< 1 $mgN.L^{-1}$), whereas ND pathway models were more suitable for systems with strong nitrite peaks (Spérandio et al., 2015).

Recently, a unified model describing the two main pathways has been proposed by Ni et al. (2014). The originality of this model is to include the description of electron transport by means of new intracellular variables. Electron donors are oxidized and produce mediated electron, then the different electron acceptors (NO, O_2, HNO_2) can compete to consume this mediated electron pool. Oxidation and reduction reactions are thus described separately (whereas they are commonly coupled in conventional activated sludge models). Consequently, in that model, the predictions depend on kinetic parameters related to intracellular variables (electron carriers) which could be difficult to assess. In contrast, the simultaneous consumption of different electron acceptors for the same donor (and the competition between them) was previously modelled using switching function. Recently Guo and Vanrolleghem (2014a) proposed to use a new expression to describe the inhibition of the nitrite reduction by oxygen, considering that oxygen plays a role in the ND pathway regulation.

Finally there is not one single way to consider two AOB pathways simultaneously in a unified approach, which still need to be confronted with experimental observations. Moreover, single or multiple pathway models have, so far, never been simultaneously confronted with NO and N_2O emissions for their validation or calibration.

Therefore the objective of this study was to evaluate a new model combining the two main AOB pathways (noted 2-P model) with the measurements of NO and N_2O emissions, placing

special emphasis on the variation of the NO/N_2O ratio. Emissions were measured in aerobic batch tests and a sequencing batch reactor (SBR), in which full nitritation and denitrification were achieved.

2 MATERIALS AND METHODS

2.1 Experimental data for model evaluation

Emissions of NO and N_2O were monitored in a sequencing batch reactor consisting of a lab-scale reactor (1.43 L of liquid) equipped with an aeration system, a mechanical stirrer (465 rpm) and a water jacket for temperature control (27.9 ± 0.5 °C). Dissolved oxygen (DO) (Hamilton), pH and oxidation-reduction potential (ORP) (Schott) were monitored. Air flow rate was imposed with a mass flowmeter. Off-gas was collected at the top of the reactor at a constant flow rate of 0.2 $L.min^{-1}$ for measurement of NO (NGA 2000 CLD from Emerson; range 0-30 ppm; minimum detectable level: 0.1 ppm) and N_2O (X-STREAM X2GP from Emerson; range: 0-100 ppm; minimum detectable level: 0.1 ppm). Data were monitored every 20 seconds. The reactor was seeded with a sludge sample from an activated sludge process with stable nitrification (wastewater treatment plant of Graulhet, France). The sludge retention time was maintained constant at 15 days. The SBR was operated with the following cycle: aerated period (nitrification), anoxic period (denitrification), settling (20 minutes) and withdrawal (8 minutes). Durations of aerobic and anoxic periods were adapted during the study in order to achieve full nitritation and denitrification. The aerobic period was initiated by feeding with ammonium-rich synthetic wastewater (403 – 445 $mgN\text{-}NH_4^+.L^{-1}$, 20 $mL.min^{-1}$, 7 – 10 min). During this period, the average pH was maintained at 8.3 ± 0.2. The anoxic period started with addition of a secondary solution (18.8 $gCOD.L^{-1}$, 6.25 $mL.min^{-1}$, 2.5 – 7.5 minutes) for full denitrification of nitrite. Throughout the study, chemical species were

quantified by ionic chromatography and standard methods after sample filtration (0.22 µm pore size filter). The concentration of free nitrous acid (HNO_2) was calculated from the nitrite concentration, temperature and pH. NO and N_2O emissions were monitored during both aerobic and anoxic phases but no significant emissions were observed in anoxic periods (checked regularly by introduction of nitrogen gas). This was certainly due to the fact that the organic carbon was perfectly dosed during denitrification. Hence only NO and N_2O peaks measured during the aerated period were analysed and the emissions were purely related to the nitrification phase as it was also checked that no heterotrophic denitrification occurred in the aerated period. For model calibration, batch kinetics were recorded specifically with various nitrite concentrations. These tests were performed in aerobic conditions with a constant air flow rate maintaining a non-limiting dissolved oxygen concentration during nitritation (2 mgO_2/L) (Table 1).

Based on NO and N_2O measurements, the gas emission rates noted NO-ER ($gN\text{-}NO.L^{-1}.h^{-1}$) and N_2O-ER ($gN\text{-}N_2O.L^{-1}.h^{-1}$) respectively were calculated using the following equations:

$N_2O\text{-}ER = [N_2O] .10^{-6}.Q_{gas}.V_m^{-1}.2.M_N.V^{-1}$

$NO\text{-}ER = [NO] .10^{-6}.Q_{gas}.V_m^{-1}.M_N.V^{-1}$

where $[N_2O]$ is the N_2O gas phase concentration (ppmv), $[NO]$ is the NO gas phase concentration (ppmv), Q_{gas} is the air flow rate ($L.h^{-1}$), V_m is the molar volume of gases ($L.mol^{-1}$), M_N is the molar mass of nitrogen ($g.mol^{-1}$), and V is the volume of the reactor (L). The total amounts of NO and N_2O emitted during an aerated period were calculated by the integration of the NO-ER and N_2O-ER. Emission factors (noted EF) are calculated as the ratio between the total amounts of NO and N_2O to the amount of ammonium removed by

nitritation. By successive measurements, the confidence intervals were estimated as 10% for N_2O emission factor and 20% for NO emission factor.

2.2 Model description

The mathematical model for AOB was developed considering both NN and ND production pathways (2-P model). A schematic description of the reactions considered is presented in Figure 1 and the stoichiometry and kinetics are presented in Tables 2 and 3 respectively. The assumptions for the description of NN and ND pathways are based on previous single pathway models (Ni et al., 2011, 2013a). The continuity of this new model was verified based on (Hauduc et al., 2010) and five processes were included in the model, corresponding to the following five enzymatic reactions: (1) NH_3 oxidation to hydroxylamine (NH_2OH) with oxygen consumption, (2) NH_2OH oxidation to nitric oxide (NO) coupled with oxygen reduction, (3) NO oxidation to nitrite (NO_2^-) coupled with oxygen reduction, (4) NO reduction to N_2O by the enzyme "Nor" coupled with the hydroxylamine oxidation to nitrite (N_2O from NN pathway), (5) HNO_2 reduction to N_2O coupled with NH_2OH oxidation to nitrite (N_2O from ND pathway). Reactions 2 and 4 describe the production of NO and N_2O respectively by the NN pathway with small corrections compared to the original model of Ni et al. (2013a) (growth takes place in reaction 2). Reaction 5 describes the N_2O production by the ND pathway. Two successive processes were considered in the original ND model (Mampaey et al., 2013; Ni et al., 2011): nitrite reduction to NO (NirK enzyme) followed by the reduction of NO to N_2O (Nor enzyme). In the present work, the decision was made to lump these two reactions together in a single process (5) corresponding to the direct reduction of nitrite to N_2O in one step. This modification was necessary to avoid the NO loop, i.e. the fact that the NO produced by the ND pathway would be rapidly oxidized to nitrite by the

nitritation process (3), as this last process has a much higher rate (Ni et al., 2014). In other words, it was assumed that the Nor enzyme rapidly consumed the nitric oxide produced by the NirK. In some situation this assumption of the amount of NO accumulated by the ND pathway was not significant (thus ignored) compared to that emitted by the NN pathway could be critical for the prediction of NO emissions. For example Kampschreur et al. (2007) reported some change in NO emission (with nitrite) which was attributed to ND pathway. In that case NO emitted by NirK could be considered (as a different state variable to avoid the NO loop). However in the present study, this was not necessary as the prediction of NO emissions was in accordance with the experimental observation, probably because at high nitrite level (case of this study) the Nor enzymes are highly synthetized and rapidly consume the intermediary NO of the ND pathway.

The ammonia oxidation rate was related to the concentration of free ammonia, which was assumed to be the true substrate of AOB (Anthonisen et al., 1976) and nitrite reduction rate was similarly related to free nitrous acid concentration. Inhibitions of AOB growth by NH_3 and HNO_2 were not considered in this work (concentrations were relatively low). A possible extension could naturally be to consider the inhibitions observed at high concentration (Law et al., 2013). The effect of dissolved oxygen on the ND pathway was considered in reaction 5 by an inhibition term as proposed by (Guo and Vanrolleghem, 2014b). This term describes the increase of the specific N_2O production rate with the decrease of DO, up to a maximum production rate, beyond which the rate decreases when DO is close to zero (Peng et al., 2015a). Note that the model was initially tested without DO inhibition (option 1), with a conventional uncompetitive inhibition term $K_i/(K_i+S)$ (option 2) and finally with the modified inhibition term (option 3). Significant improvement was observed with the third option especially for the prediction of long term data (SBR) at relatively low DO (1-2 mg/L). This comparison can be found in Supplementary Information (S4). However it should be noted that

this is not a generic conclusion as the experimental design was more focused on the nitrite effect in this study. Such assumption would need more strong evidence with future work dedicated to DO effect. The gas liquid transfers of oxygen, NO and N_2O were also included in the models. The transfer coefficients (K_La) for NO and N_2O were calculated with the measured oxygen transfer coefficient and the respective diffusivity ratio (Ye et al., 2014).

2.3 Model simulation, calibration and sensitivity analysis

All the simulations, sensitivity analysis and calibration were performed with AQUASIM software (Reichert, 1998). A relative-relative sensitivity function was determined for each parameter and measured variable in order to assess the identifiability of model parameters (identifiability analysis). Furthermore, the derivatives calculated in sensitivity analyses allowed to estimate the uncertainty in parameter estimates considering experimental uncertainty (5% for ammonia, nitrite, dissolved oxygen, 10% for gas measurements). Analysis was performed considering the simulations of batch experiments presented in Table 1 simultaneously.

In this study the 2-P model was compared to other models developed previously. Above all, the main goal was to find out which model was able to simultaneously describe the variation of N_2O and the variation of the tendency of NO/N_2O ratio. Different single pathway models based on the ND (Guo and Vanrolleghem, 2014a; Mampaey et al., 2013; Ni et al., 2011; Pocquet et al., 2013) or NN pathway (Ni et al., 2013a) were tested (Supplementary Information, Table S1, S2, S3, S4, S5). Finally the 2-P model developed in this study was also compared to the unified model proposed by Ni et al. (2014). The same approach was used for all the models tested. First the model was calibrated on batch tests (Table 1). Then the calibrated model was evaluated and possibly validated by simulating the long-term data collected on the SBR, i.e. for 187 cycles. During the whole experimental period (6 months),

variations of ammonia feeding conditions and pH led to a variation of the nitrite and free nitrous acid accumulated in the reactor. Moreover the dissolved oxygen concentration also varied (from 1 to 5.5 mg/L) depending on both nitrification rate and air flow rate.

The 2-P model includes fourteen independent parameters. The maximum kinetic rates noted "q" (for processes without growth 1, 3, 4, 5) were not determined independently but related to the maximum growth rate 'μ' (related to process 2). Indeed maximum rates are potentially linked to the same specific enzymes (reactions 2, 3, 4, 5, are linked to HAO coupled with different electron acceptors). The value of $q_{AOB,HAO}$ was calculated as the growth rate $\mu_{AOB,HAO}$ divided by Y_{AOB}, leading to a similar substrate utilization rate for reactions 2 and 3 both related to the HAO oxidation activity with oxygen as electron acceptors. The maximum rates of reactions 4 and 5 are related to HAO coupled with nitric oxide and nitrite reduction respectively. Thus the maximum rates $q_{AOB,N2O,NN}$ and $q_{AOB,N2O,ND}$ were calculated by multiplying $q_{AOB,HAO}$ by two different reduction factors noted $\eta_{AOB,NN}$ and $\eta_{AOB,ND}$ respectively. Note that these coefficients are not called "anoxic" reduction factors as the reactions are still active in presence of oxygen. Note also that the values of these reduction factors cannot be compared directly to those of previous models by (Ni et al., 2011) and (Ni et al., 2013b) as they were originally applied to the growth rate.

3 RESULTS

3.1 Parameter calibration and sensitivity analysis

The results from sensitivity analysis are presented in Table 4. The set of parameter values (and uncertainties) identified for the two pathway model is presented in Table 5 (All the data concerning the other models are given in the supplementary information). Three parameters were directly implemented with values from literature (Y_{AOB}, $i_{N,BM}$, μ_{AOB}). The other

parameters were estimated by successive calibrations with the different measured variables. Based on sensitivity analysis, the parameters influencing ammonium uptake rate and oxygen consumption were firstly calibrated (i.e. parameters related to AMO and HAO reactions) with NH_4^+, NO_2^- and O_2 measurements. Then the parameters influencing specifically the N_2O and NO emissions (related to both rate 4 and rate 5) were adjusted based on experimental N_2O and NO measurements in the gas phase. Based on the sensitivity analysis, it was found that N_2O emission was more specifically influenced by the factors related to rate 5 ($\eta_{AOB,ND}$, $K_{O2,AOB,ND}$, $K_{I,O2,AOB,ND}$, $K_{HNO2,AOB}$) which seems logical as the ND was the major pathway contributing to N_2O emissions in this study. A previous analysis (Pocquet el al., 2013) demonstrated that the correlation between the key parameters of ND pathway ($\eta_{AOB,NN}$ and K_{HNO2}) during the estimation was minimized thanks to the use of data obtained in a large range of nitrite concentration, as applied in this study. The predicted NO was very sensitive to parameters related to HAO ($K_{NH2OH,AOB}$, $K_{O2,AOB,2}$, $K_{NO,AOB,HAO}$) and slightly sensitive to parameter related to NN pathway i.e. rate 5 ($\eta_{AOB,NN}$). Thus the use of NO measurement for calibration logically improved the identifiability of those parameters. Finally efficient parameter identification was obtained by calibrating the model successively on the different type of measurements (soluble compounds, NO and N_2O) using simultaneously a relatively high number of data. Most of the estimated parameters showed a satisfying accuracy (table 5) except those with poor influence of the simulations.

3.2 Modelling batch experiments with the 2-P model

The 2-P model was initially calibrated with a series of batch tests with similar ammonia concentrations but different initial nitrite concentrations. Figure 2 presents typical results obtained during four experiments (ammonia injection at 1 minute). Figure 3 shows the experimental data and simulations obtained for the emission factor N_2O-EF and the NO/N_2O

ratio for all batch experiments presented in Table 1. During all experiments, nitrate concentration was negligible and ammonia was fully converted to nitrite. The SBR process had been operating for 3 months before these tests with appropriate aeration phase control to eliminate the NOB activity. The ammonium, nitrite and dissolved oxygen concentrations were correctly described by the 2-P model. Before calibrating the NO and N_2O productions, a good prediction of DO and nitrite was crucial considering their combined effect.

As shown in Figure 2, the 2-P model accurately predicted the dynamics of N_2O emissions, and the effect of nitrite on the emissions. By comparing the different responses on Figure 2 (a, b and c), in the beginning 2 min, N_2O (ppm) is very small, only NO is produced increasingly, resulting in a sharp increase of NO/N_2O ratio in the beginning. After 2 min, N_2O production starts and its production rate is faster than NO (Figure 2-a), which causes a sudden decrease of NO/N_2O ratio. This phenomenon was especially observed when nitrite concentration was low or null initially. Then, when ammonia was depleted, N_2O starts to decrease and gets zero after a few minutes (NO/N_2O ratio was not calculated in that final zone due to high uncertainty). As indicated by the figure 2-d (NN and ND contribution to N_2O emission), the model predicted that ND was the major pathway responsible for N_2O emission, and the N_2O emission rate was stimulated by the increase of free nitrous acid (HNO_2) concentration (or nitrite). Hence the agreement between simulated N_2O and experimental N_2O was mainly related to the ND pathway prediction (process 5). In contrast, NO emissions were quantitatively much lower than N_2O emissions and NO reached its maximum concentration before N_2O. The 2-P model gave an acceptable prediction of NO emissions and the prediction of NO/N_2O matched experimental data well. In the 2-P model, the variation of the NO/N_2O ratio was basically related by the variation of ND and NN contributions to the N_2O emissions. NO was rapidly emitted by hydroxylamine oxidation (process 2), and N_2O was firstly produced by process 4 (NN pathway) independently of the presence of nitrite. Then N_2O was

produced by process 5 (ND pathway) consuming hydroxylamine and nitrite, which led to the decrease of the NO/N_2O ratio. This progressive stimulation of the ND pathway during batch kinetics was in agreement with the data from isotope signature analysis reported in literature (Wunderlin et al., 2013).

As shown in Figure 3a, the N_2O emissions clearly increased proportionally to nitrite concentration (the same correlation was observed with free nitrous acid as the pH was similar during these tests). It was checked that this increase was completely reversible by repeating a test at low nitrite level at the end of the series. In contrast, the variations of NO emission factors were not statistically significant. Consequently, the NO/N_2O ratio decreased with the increase of nitrite (Figure 3b). For these different experiments the two pathway model predicted the increase of the N_2O emission factor and the decrease of the $NO\text{-}EF/N_2O\text{-}EF$ ratio, consistently with experimental observations (Figure 3.a and 3.b respectively). The predictions of the 2-P model indicate that the increase of free nitrous acid or nitrite stimulated N_2O emission by the ND pathway and consequently the decrease of the NO/N_2O ratio. The level of HNO_2 for which the decrease of the $NO\text{-}EF/N_2O\text{-}EF$ ratio was observed was slightly underestimated by the model. However, except for this small discrepancy, the trend of the simulation was comparable to observations. The $NO\text{-}EF/N_2O\text{-}EF$ ratio decreased from 0.5 to less than 0.02 for the range of HNO_2 explored (0.02 – 0.95 $\mu gN.L^{-1}$). The highest ratio was obtained when the contribution of the NN pathway was maximum (at low HNO_2) whereas the lowest ratio was predicted when ND was the major contributing pathway (at the highest HNO_2). Basically the ability of the model to describe NO emission uncorrelated to nitrite accumulation was due to the fact that NO was considered to be only emitted by hydroxylamine oxidation, neglecting the possible contribution of the ND pathway. Even if this assumption is a simplification of the reality it enabled the observations to be reasonably well described. However this assumption should not be considered as a general statement (it

probably depends on the level of activation of NirK and Nor enzymes). And it should be noted that the model was not confronted to a system with important variation of NO emission.

3.3 Validation of the 2-P model with long-term data set from SBR process

Simulations were compared with the long-term data set collected in the SBR (Figure 4). N_2O-EF, NO-EF and NO-EF/N_2O-EF ratio were calculated for each cycle based on the off-gas measurements during the aerated phase. The data are represented in Figure 4 versus the maximum HNO_2 concentration reached during the aerated period of the cycle, variation of HNO_2 resulting in both nitrite and pH variations. The time evolution during the long-term validation with both nitrite and DO variations are also provided in supplementary information (figure S6, S7). Each point corresponds to the emission factor calculated for one cycle (187 cycles). The data confirmed the correlation between N_2O emissions and HNO_2 accumulation (Figure 4.a). For HNO_2 concentrations below 0.60 $\mu gN.L^{-1}$ the N_2O-EF remained lower than 1% for most of the cycles. The N_2O-EF increased significantly up to 3% for an HNO_2 concentration of 0.8 $\mu gN.L^{-1}$. Values ranging from 4% to more than 11% were finally observed for HNO_2 accumulation close to 0.9 $\mu gN.L^{-1}$ and it should be noted that the dissolved oxygen was observed to vary during the corresponding period. The highest emission factors were observed for relatively low DO (1-1.5 mg/L) in that period. For comparison, in a previous batch test, the emission factor was 4.5% at similar HNO_2 level with DO higher than 2-2.5 mgO_2/L (Figure 3). In contrast NO emission varied from 0.024% to 0.078% but was not correlated with HNO_2 concentration (Figure 4.b). In consequence, the NO-EF/N_2O-EF ratio decreased from 0.20 to 0.002 gN-NO/gN-N_2O for an HNO_2 concentration increase from 0.24 to 0.92 $\mu gN.L^{-1}$ (Figure 4.c). This result is thus similar to those previously observed for specific batch experiments (figure 3).

The simulations obtained with the 2-P model were in agreement with the experimental observations for N_2O-EF, NO-EF and NO-EF/N_2O-EF ratio. The calibrated model was capable of predicting most of the data collected during 6 months on the SBR, with a large range of N_2O emissions factors from 0.1% (at low nitrite, high DO) to 8% (at high nitrite, low DO). The model slightly underestimated the N_2O emissions for a 4 day period with rapid aerobic-anoxic alternance (at low DO), this high frequency may have generated an additional emission during anoxic period that we did not consider in the model. The increase of the N_2O emission factor as a function of HNO_2 was predicted very correctly (only the highest N_2O-EF obtained during those 4 days were slightly under-estimated). In addition the N_2O production was exacerbated when high nitrite and low DO were maintained simultaneously. This effect of DO was described by the model thanks to the modified inhibition term on DO (see Supplementary Information figure S5). It is important to note, here, that the 2-P model predicted a 6 month period with 187 cycles obtained at different pH and different DO (1 to 6 mg/L). Compared to batch experiments, the variation of HNO_2 resulted from simultaneous variations of pH and nitrite. This result validates the choice of using free nitrous acid in the kinetic expressions of the model.

Basically, the 2-P model has similar predictive capacities as the NN pathway model for NO-EF (Figure S3 in supplementary information). Finally, the 2-P model made it possible to explore the relative contribution of both NN and ND pathways to the N_2O emissions (Figure 4.d). The model predicted a major contribution of the ND pathway, which increased from 80% to 99% with the increase of the HNO_2 concentration from 0.24 to 0.92 $\mu gN.L^{-1}$.

3.4 Simulations with other existing models

The predictions of different single pathway models were also confronted with both NO and N_2O emissions collected in this study. The main conclusions were that single pathway models

were not able to predict NO and N_2O profiles simultaneously. The ND pathway model gave a satisfactory description of N_2O but did not capture NO trends. Conversely, the model based on the NN pathway correctly described NO emissions but did not match the N_2O trend (see supplementary information, Figures S1 and S2). As shown by Figure 3a, for different batch experiments at various nitrite concentrations, the ND model correctly predicted the increase of N_2O emission whereas the NN model was not able to predict any influence of nitrite. In addition, both NN and ND models predicted a constant ratio between NO and N_2O, which was not confirmed by experimental observations (Figure 3b). Basically, the NO and N_2O productions are structurally related in single pathway model and it is not possible to predict a significant variation of NO/N_2O ratio. Finally, only the simulations obtained with the 2-P model were consistent with the experimental observations.

The results were also compared to the predictions of the model recently proposed by Ni et al. (2014) based on multiple production pathways and intracellular electron carriers. The model was combined with gas liquid transfer equations and batch experiments were simulated (see Figure S4 in supplementary information). With original calibration, this model predicted NO emissions higher than N_2O emissions, which was not in agreement with our observation and those mentioned in the literature (Ahn et al., 2011; Kampschreur et al., 2008; Rodriguez-Caballero and Pijuan, 2013). In fact, the multiple pathway model was initially developed without modelling NO stripping by Ni et al. (2014) assuming that the NO consumption mainly occurred inside AOB cells without any bulk accumulation (or emission). For this reason, this multiple pathway model should be considered with more attention if the objective is to predict realistic NO emissions in the gas phase. In its present form it was possible only after considerable calibration effort, but these changes could completely modify the prediction capabilities of the model concerning other compounds. To conclude, more work would be

necessary to evaluate whether both the NO and the N_2O emissions could be described appropriately with Ni's multiple pathway model or not.

4 DISCUSSION

4.1. Capabilities of two pathway model to predict NO and N_2O emissions and pathway regulation

The two pathway model developed in this work is to date the only model that has been validated on both NO and N_2O measurements monitored during batch experiences experiments and long long-term operation of an SBR. The 2-P model successfully predicts the variation of the NO/N_2O ratio as well as the emission factors. The variation of the NO/N_2O ratio predicted by the model is related to a variation of the contribution of each pathway in the N_2O production, the maximum NO/N_2O ratio being predicted when the N_2O is produced by the NN pathway.

The 2-P model predicts a dynamic variation of the contribution of each pathway to the N_2O emissions as shown in Figure 5 (simulation of a batch experiment). Initially the contribution of the ND pathway accounted for about 60% but increased rapidly, reaching 100% at the end. This is in full agreement with the studies based on measurement of the site preference (SP) in isotopomers of N_2O to distinguish the pathways (Peng et al., 2014; Toyoda et al., 2011; Wunderlin et al., 2013). In similar batch experiments, Wunderlin et al. (2013) found that the contribution of the ND pathway increased with time from around 75% to 100%. The same authors also demonstrated that the contribution of the NN pathway was dominant when hydroxylamine was used as the nitrogen source, and the 2-P model also predicts a maximum contribution by the NN process in case of hydroxylamine injection associated with high NO accumulation (not shown). On the one hand, the N_2O production rate through the ND pathway

increases with time in relation with nitrite (or HNO_2). On the other hand, the N_2O produced by the NN pathway is stimulated by hydroxylamine and NO accumulation due to the unbalanced situation observed between AMO and HAO reaction rates in batch conditions. As NO was assumed to be mainly related to that hydroxylamine oxidation (HAO) in the model, it was not influenced by nitrite. This explains the decrease of the NO/N_2O ratio with time and with nitrite accumulation. In absence of nitrite (no accumulation at all, or if the ND pathway is artificially switched off), the calibrated model predicts an NO/N_2O ratio close to 0.6 for pure production by the NN pathway. Therefore the model tends to confirm the possible relation between NO/N_2O and pathway contributions, which still need to be further demonstrated in future work. Finally the capability of the 2-P model for predicting N_2O emissions was demonstrated in that study but more work would be necessary to demonstrate that capability for predicting fluctuation of NO emissions. Further analysis of NN and ND contributions to NO emission with isotope analysis may be used to confirm the assumptions related to NO emission pathway.

4.2 Combined effect of operating parameters on emissions

In this work, the experimental data indicated that N_2O emission rate and emission factor were correlated to the variations of nitrite, pH, and dissolved oxygen. The effect of nitrite and pH were combined in the model by the use of free nitrous acid as the substrate for AOB denitrification. In the range of pH explored in the SBR, good agreement was observed. The variations of N_2O emissions with nitrite or slight pH change were predicted correctly by the model.

Peng et al., (2015) recently demonstrated the combined effect of DO and nitrite on the N_2O emission and pathway regulation. A simulation of the influence of HNO_2 and DO on NO and N_2O emission factors, $NO\text{-}EF/N_2O\text{-}EF$ ratio, and the contribution of pathways is presented in

Figure 6. The simulations based on the 2-P model confirm a combined effect of HNO_2 and DO on the N_2O emission pathways. For a constant DO (2 $mgO_2.L^{-1}$), an increase in the HNO_2 concentration leads to an increase in the N_2O emission factor, an increase in the ND contribution and a decrease in the NO-EF/N_2O-EF ratio. For a similar HNO_2 concentration (0.7 $\mu gN\text{-}HNO_2.L^{-1}$) the increase of DO leads to a decrease of the N_2O-EF, a small decrease of the ND contribution associated with a small increase of the NN contribution, and a slight increase of the NO-EF/N_2O-EF. This effect of DO is in good agreement with the recent work of (Peng et al., 2014), who found that the ND pathway was the main contributor to N_2O production during ammonia oxidation (95% - 73% of N_2O from the ND pathway) and that an increase of the dissolved oxygen (DO) concentration from 0.2 to 3 $mgO_2.L^{-1}$ led to an increase of the NN pathway contribution from 5% to 27%. Finally, the highest predicted N_2O emission factors are observed for high HNO_2 concentration and relatively low DO (0.5-1 mgO_2/L). This is also in good agreement with our practical observations as the maximal peak in the SBR process was observed when high HNO_2 (0.9µgN/L) occurred at the same time as low DO (1.0 mg/L). This is also in good agreement with the study by Peng et al., (2015) on the combined effect of DO and nitrite. As the independent effect of DO was not fully tested in this work (more focused on nitrite effect) conclusion about oxygen effect should be considered with caution. A future analysis will be dedicated to the confrontation of 2-P models on data with combined DO and nitrite effect.

4.3 Comparison of the 2-P model with other existing models and future use of the models

None of the AOB models based on a single pathway were able to describe the NO/N_2O ratio variation obtained experimentally. Moreover multiple pathway models were able to describe a difference in the effect of an operating parameter (DO for example) depending on the contribution of the pathway. For that reason the use of single pathway models should be

limited to a given zone of experimental conditions. Peng et al. (2015b) recently tested the predictive ability of a single pathway model to describe the N_2O data generated by a multiple pathway model. The conclusion was that the AOB denitrification model can be applied at low DO (<0.5 mg/L) or at high DO with significant nitrite accumulation (DO > 0.5 and NO_2^- > 1 mg N/L). The latter situation corresponds to the present work and our study confirms that the ND model was the best single pathway model to describe N_2O emission. This is logical as the contribution of this pathway to N_2O emission has been demonstrated to be major in the conditions of this study, due to the significant accumulation of nitrite. However it was also shown that the 2-P model was much better for predicting N_2O emissions as well as NO tendency. It was expected that the ND model would not be able to describe N_2O emissions in a system with low nitrite level (high NOB activity), leading to N_2O emissions by the NN pathway (Ni et al., 2013b). As previously demonstrated, ND models (Guo and Vanrolleghem, 2014a; Mampaey et al., 2013; Pocquet et al., 2013) were able to describe experimental data in different systems but needed a significant and sometimes unrealistic adjustment of key parameters (η_{AOB}) to be able to describe a system with a low nitrite level (Spérandio et al., 2015). This was probably needed to compensate for the fact that the hydroxylamine pathway was not considered.

In contrast, in this study, it was shown that the NN model was capable of describing the NO emissions but did not match the N_2O emissions. The calibration of the two pathway model indicated that the N_2O emission rate (and emission factor) due to the NN pathway was likely to be low in the reactor studied. Indeed the maximum specific rate for N_2O production by the NN pathway ($q_{AOB,N2O,NN}$ in Table 4) was 3.10^{-4} mgN.mgCODX^{-1}.h^{-1}, i.e. 180 times lower than the maximum specific rate for N_2O production by the ND pathway ($q_{AOB,N2O,ND}$ = 0.0542 mgN.mgCODX^{-1}.h^{-1}). The last rate was also 4 times lower than the maximum specific rate of HAO reaction with oxygen ($q_{AOB,HAO}$=0.2167 mgN.mgCODX^{-1}.h^{-1}). Consequently, during a

typical ammonia batch experiment, predictions indicated that about 96.7% of N_2O would be produced by the ND pathway and only 3.3% by the NN pathway. The last study by Peng et al. (2015b) suggested that the hydroxylamine oxidation model could be applied under high DO (DO>1.5mg/L) and nitrite concentration between 0 and 5.0 mgN/L. Our study revealed that, in a larger range of nitrite concentrations, this model was not able to predict the observations. Finally the model proposed in this study was also compared to the multiple pathway model recently proposed by Ni et al. (2014). Further work would be necessary to compare the predictive abilities of these two approaches. Our first comparison indicates that comparable prediction of N_2O emissions could be obtained but the 2-P model proposed in this study gave more realistic predictions for NO emissions, in agreement with experiments and previous literature (Ahn et al., 2011; Kampschreur et al., 2008; Rodriguez-Caballero and Pijuan, 2013). This is possibly due to the fact that the variable NO in the electron based model is likely to represent a local intracellular concentration instead of the concentration present in the bulk (which would be lower). Additional work will be necessary to determine which of these different concepts would be recommended for use in each specific situation. NO measurements from different experimental systems could be useful in order to test the proposed models and evaluate more in deep their ability to predict NO emission.

5 CONCLUSION

- A two pathway model was successfully calibrated on both N_2O and NO emissions measured during batch experiments and SBR operation. The model accurately predicted the effect of nitrite (via free nitrous acid) and was validated on long-term data collected at variable values of dissolved oxygen and pH. The simulated effects of nitrite and dissolved oxygen on pathway regulation were in agreement with the literature.

- The 2-P model was able to describe the decrease of NO/N_2O ratio with HNO_2 accumulation whereas none of the models based on a single pathway could do so. The decrease in NO/N_2O ratio was explained by an increased contribution of the nitrifier denitrification pathway (ND), which was the dominant pathway in the system studied. Inversely, the highest NO/N_2O corresponded to the situation of maximal contribution of the hydroxylamine pathway (NN). Thus measurement of the NO/N_2O ratio was a useful tool for calibrating the multiple pathway model.

6 ACKNOWLEGEMENTS

Mathieu Pocquet was financially supported by the French National Research Agency (ANR) and the project was co-funded by Région Midi-Pyrénées. The authors would like to thank E. Mengelle, M. Bounouba and D. Delagnes for their contributions.

7 REFERENCES

Ahn, J.H., Kwan, T., Chandran, K., 2011. Comparison of Partial and Full Nitrification Processes Applied for Treating High-Strength Nitrogen Wastewaters: Microbial Ecology through Nitrous Oxide Production. Environ. Sci. Technol. 45, 2734–2740. doi:10.1021/es103534g

Anthonisen, A.C., Loehr, R.C., Prakasam, T.B.S., Srinath, E.G., 1976. Inhibition of Nitrification by Ammonia and Nitrous Acid. J. Water Pollut. Control Fed. 48, 835–852. doi:10.2307/25038971

Chandran, K., Stein, L.Y., Klotz, M.G., van Loosdrecht, M.C.M., 2011. Nitrous oxide production by lithotrophic ammonia-oxidizing bacteria and implications for engineered nitrogen-removal systems. Biochem. Soc. Trans. 39, 1832–1837. doi:10.1042/BST20110717

Crutzen, P.J., 1979. The Role of NO and NO2 in the Chemistry of the Troposphere and Stratosphere. Annu. Rev. Earth Planet. Sci. 7, 443–472. doi:10.1146/annurev.ea.07.050179.002303

Daelman, M.R.J., van Voorthuizen, E.M., van Dongen, L.G.J.M., Volcke, E.I.P., van Loosdrecht, M.C.M., 2013. Methane and nitrous oxide emissions from municipal wastewater treatment - results from a long-term study. Water Sci. Technol. J. Int. Assoc. Water Pollut. Res. 67, 2350–2355. doi:10.2166/wst.2013.109

Fischedick, M., Roy, J., Abdel-Aziz, A., Acquaye, A., Allwood, J.M., Ceron, J.-P., Geng, Y., Kheshgi, H., Lanza, A., Perczyk, D., Price, L., Santalla, E., Sheinbaum, C., Tanaka, K., 2014. Industry, in: Climate Change 2014: Mitigation of Climate Change. Contribution of Working Group III to the Fifth Assessment Report of the Intergovernmental Panel on Climate Change [Edenhofer, O., R. Pichs-Madruga, Y. Sokona, E. Farahani, S. Kadner, K. Seyboth, A. Adler, I. Baum, S. Brunner, P. Eickemeier, B. Kriemann, J. Savolainen, S. Schlömer, C. von Stechow, T. Zwickel and J.C. Minx (eds.)]. Cambridge University Press, Cambridge, United Kingdom and New York, NY, USA.

Guo, L., Vanrolleghem, P.A., 2014a. Full-scale simulation of N2O emissions with ASMG2d and elucidation of its different production and emission sources in nitrogen (N) and phosphorus (P) removed systems. Rev.

Guo, L., Vanrolleghem, P.A., 2014b. Calibration and validation of an activated sludge model for greenhouse gases no. 1 (ASMG1): prediction of temperature-dependent N2O emission dynamics. Bioprocess Biosyst. Eng. doi:10.1007/s00449-013-0978-3

Hauduc, H., Rieger, L., Takács, I., Héduit, A., Vanrolleghem, P.A., Gillot, S., 2010. A systematic approach for model verification: application on seven published activated sludge models. Water Sci. Technol. 61, 825. doi:10.2166/wst.2010.898

Henze, M., 2000. Activated Sludge Models: ASM1, ASM2, ASM2d and ASM3. IWA Publishing.

Hiatt, W.C., Grady, C.P.L., 2008. An Updated Process Model for Carbon Oxidation, Nitrification, and Denitrification. Water Environ. Res. 80, 2145–2156. doi:10.2175/106143008X304776

Kampschreur, M.J., Temmink, H., Kleerebezem, R., Jetten, M.S.M., Van Loosdrecht, M.C.M., 2009. Nitrous oxide emission during wastewater treatment. Water Res. 43, 4093–4103. doi:10.1016/j.watres.2009.03.001

Kampschreur, M.J., van der Star, W.R.L., Wielders, H.A., Mulder, J.W., Jetten, M.S.M., van Loosdrecht, M.C.M., 2008. Dynamics of nitric oxide and nitrous oxide emission during full-scale reject water treatment. Water Res. 42, 812–826. doi:10.1016/j.watres.2007.08.022

Kim, S.-W., Miyahara, M., Fushinobu, S., Wakagi, T., Shoun, H., 2010. Nitrous oxide emission from nitrifying activated sludge dependent on denitrification by ammonia-oxidizing bacteria. Bioresour. Technol. 101, 3958–3963. doi:10.1016/j.biortech.2010.01.030

Law, Y., Lant, P., Yuan, Z., 2013. The confounding effect of nitrite on N2O production by an enriched ammonia-oxidizing culture. Environ. Sci. Technol. 47, 7186–7194. doi:10.1021/es4009689

Law, Y., Ni, B.-J., Lant, P., Yuan, Z., 2012. N2O production rate of an enriched ammonia-oxidising bacteria culture exponentially correlates to its ammonia oxidation rate. Water Res. 46, 3409–3419. doi:10.1016/j.watres.2012.03.043

Mampaey, K.E., Beuckels, B., Kampschreur, M.J., Kleerebezem, R., van Loosdrecht, M.C.M., Volcke, E.I.P., 2013. Modelling nitrous and nitric oxide emissions by autotrophic ammonia-oxidizing bacteria. Environ. Technol. 34, 1555–1566.

Ni, B.-J., Peng, L., Law, Y., Guo, J., Yuan, Z., 2014. Modeling of nitrous oxide production by autotrophic ammonia-oxidizing bacteria with multiple production pathways. Environ. Sci. Technol. 48, 3916–3924. doi:10.1021/es405592h

Ni, B.-J., Ruscalleda, M., Pellicer-Nàcher, C., Smets, B.F., 2011. Modeling nitrous oxide production during biological nitrogen removal via nitrification and denitrification: extensions to the general ASM models. Environ. Sci. Technol. 45, 7768–7776. doi:10.1021/es201489n

Ni, B.-J., Ye, L., Law, Y., Byers, C., Yuan, Z., 2013b. Mathematical Modeling of Nitrous Oxide (N2O) Emissions from Full-Scale Wastewater Treatment Plants. Environ. Sci. Technol. 47, 7795–7803. doi:10.1021/es4005398

Ni, B.-J., Yuan, Z., Chandran, K., Vanrolleghem, P.A., Murthy, S., 2013a. Evaluating four mathematical models for nitrous oxide production by autotrophic ammonia-oxidizing bacteria. Biotechnol. Bioeng. 110, 153–163. doi:10.1002/bit.24620

Peng, L., Ni, B.-J., Erler, D., Ye, L., Yuan, Z., 2014. The effect of dissolved oxygen on N2O production by ammonia-oxidizing bacteria in an enriched nitrifying sludge. Water Res. 66, 12–21. doi:10.1016/j.watres.2014.08.009

Peng, L., Ni, B.-J., Ye, L., Yuan, Z., 2015a. The combined effect of dissolved oxygen and nitrite on N2O production by ammonia oxidizing bacteria in an enriched nitrifying sludge. Water Res. 73, 29–36. doi:10.1016/j.watres.2015.01.021

Peng, L., Ni, B.-J., Ye, L., Yuan, Z., 2015b. Selection of mathematical models for N2O production by ammonia oxidizing bacteria under varying dissolved oxygen and nitrite concentrations. Chem. Eng. J. 281, 661–668. doi:10.1016/j.cej.2015.07.015

Pocquet, M., Queinnec, I., Spérandio, M., 2013. Adaptation and identification of models for nitrous oxide (N2O) production by autotrophic nitrite reduction. Proc. 11th IWA Conf. Instrum. Control Autom. ICA2013 Narbonne, France, September 18-20.

Reichert, P., 1998. User manual, computer program for the identification and simulation of aquatic systems.

Rodriguez-Caballero, A., Pijuan, M., 2013. N2O and NO emissions from a partial nitrification sequencing batch reactor: exploring dynamics, sources and minimization mechanisms. Water Res. 47, 3131–3140. doi:10.1016/j.watres.2013.03.019

Spérandio, M., Pocquet, M., Guo, L., Ni, B.-J., Vanrolleghem, P.A., Yuan, Z., 2015. Calibration of five candidate nitrous oxide production models with four continuous long-term wastewater treatment process data series. Bioprocess Biosyst. Eng.

Stein, L.Y., 2011. Surveying N2O-producing pathways in bacteria. Methods Enzymol. 486, 131–152. doi:10.1016/B978-0-12-381294-0.00006-7

Toyoda, S., Suzuki, Y., Hattori, S., Yamada, K., Fujii, A., Yoshida, N., Kouno, R., Murayama, K., Shiomi, H., 2011. Isotopomer analysis of production and consumption mechanisms of N2O and CH4 in an advanced wastewater treatment system. Environ. Sci. Technol. 45, 917–922. doi:10.1021/es102985u

Wunderlin, P., Lehmann, M.F., Siegrist, H., Tuzson, B., Joss, A., Emmenegger, L., Mohn, J., 2013. Isotope signatures of N2O in a mixed microbial population system: constraints on N2O producing pathways in wastewater treatment. Environ. Sci. Technol. 47, 1339–1348. doi:10.1021/es303174x

Wunderlin, P., Mohn, J., Joss, A., Emmenegger, L., Siegrist, H., 2012. Mechanisms of N2O production in biological wastewater treatment under nitrifying and denitrifying conditions. Water Res. 46, 1027–37.

Ye, L., Ni, B.-J., Law, Y., Byers, C., Yuan, Z., 2014. A novel methodology to quantify nitrous oxide emissions from full-scale wastewater treatment systems with surface aerators. Water Res. 48, 257–268. doi:10.1016/j.watres.2013.09.037

Zumft, W.G., 1993. The biological role of nitric oxide in bacteria. Arch. Microbiol. 160, 253–264. doi:10.1007/BF00292074

Table 1. Batch experiments with ammonium addition for different nitrite concentrations. Constant flow rate and DO during nitrification phase.

Experiment	Initial NH_4^+ injected ($mgN.L^{-1}$)	NO_2^- ($mgN.L^{-1}$)		HNO_2 ($\mu gN.L^{-1}$)		EF ($gN\text{-}NxO/gN\text{-}NHx$)		NO/N_2O
		Start	End	Start	End	N_2O	NO	(gN/gN)
1	10.5	10.5	21.0	0.00	0.15	0.16%	0.0811%	0.516
2	10.5	22.5	33.0	0.00	0.16	0.12%	0.0484%	0.405
3	10.5	20.5	31.0	0.15	0.22	0.83%	0.0805%	0.097
4	10.5	36.5	47.0	0.20	0.28	0.89%	0.0475%	0.053
5	10.5	68.5	79.0	0.34	0.57	2.61%	0.0814%	0.031
6	10.5	112.5	123.0	0.61	0.95	4.58%	0.0770%	0.017

Table 2. Stoichiometry of the 2 pathway model (Gujer matrix).

Process	Model Components – 2-P model						
	S_{NH}	S_{NH_2OH}	S_{NO}	$S_{NO_2^-}$	S_{N_2O}	S_{O_2}	X_{AOB}
1	-1	1				$-8/7$	
2	$-i_{N,BM}$	$-1/Y_{AOB}$	$1/Y_{AOB}$			$-\left(12/7 - Y_{AOB}\right)/Y_{AOB}$	1
3			-1	1		$-4/7$	
4		-1	-4	1	4		
5		-1		-1	2		

Table 3. Kinetics of the 2-P model.

Process	Kinetic rate expressions – 2-P model
1	$q_{AOB,AMO} \frac{S_{O_2}}{S_{O_2} + K_{O_2,AOB,1}} \frac{S_{NH_3}}{S_{NH_3} + K_{NH_3,AOB}} X_{AOB}$
2	$\mu_{AOB,HAO} \frac{S_{O_2}}{S_{O_2} + K_{O_2,AOB,2}} \frac{S_{NH_2OH}}{S_{NH_2OH} + K_{NH_2OH,AOB}} X_{AOB}$*
3	$q_{AOB,HAO} \frac{S_{O_2}}{S_{O_2} + K_{O_2,AOB,2}} \frac{S_{NO}}{S_{NO} + K_{NO,AOB,HAO}} X_{AOB}$
4	$q_{AOB,N_2O,NN} \frac{S_{NH_2OH}}{S_{NH_2OH} + K_{NH_2OH,AOB}} \frac{S_{NO}}{S_{NO} + K_{NO,AOB,NN}} X_{AOB}$
5	$q_{AOB,N_2O,ND} \frac{S_{NH_2OH}}{S_{NH_2OH} + K_{NH_2OH,AOB}} \frac{S_{HNO_2}}{S_{HNO_2} + K_{HNO_2,AOB}} f(S_{O2}).X_{AOB}$
	With $f(S_{O2}) = \frac{S_{O_2}}{K_{O_2,AOB,ND} + \left(1 - 2 \cdot \sqrt{K_{O_2,AOB,ND} / K_{I,O_2,AOB}}\right) \cdot S_{O_2} + S_{O2}^2 / K_{I,O_2,AOB}}$

* In process 2, growth limitation by ammonium is mathematically imposed with $S_{NH}/(S_{NH}+10^{-12})$

Table 4. Result from sensitivity analysis. Parameters with sensitivity function higher than 5% (relative-relative).

Processes	Measured variables				Other variables		
	S_{NH}	S_{O2}	NO_{gas}	N_2O_{gas}	S_{NH2OH}	N_2O_{NN}	N_2O_{ND}
General	μ_{AOB} Y_{AOB}	μ_{AOB} Y_{AOB}	μ_{AOB} Y_{AOB}	μ_{AOB} Y_{AOB}	μ_{AOB} Y_{AOB}	μ_{AOB} Y_{AOB}	μ_{AOB} Y_{AOB}
AMO	$K_{O2,AOB,1}$ $K_{NH3,AOB}$	$K_{O2,AOB,1}$	$K_{O2,AOB,1}$ $K_{NH3,AOB}$	$K_{O2,AOB,1}$ $K_{NH3,AOB}$	$K_{O2,AOB,1}$ $K_{NH3,AOB}$	$K_{O2,AOB,1}$ $K_{NH3,AOB}$	$K_{O2,AOB,1}$ $K_{NH3,AOB}$
HAO	$K_{NH2OH,AOB}$	$K_{NH2OH,AOB}$	$K_{NH2OH,AOB}$ $K_{O2,AOB,2}$ $K_{NO,AOB,HAO}$	$K_{NH2OH,AOB}$ $K_{O2,AOB,2}$	$K_{NH2OH,AOB}$ $K_{O2,AOB,2}$	$K_{NH2OH,AOB}$ $K_{O2,AOB,2}$ $K_{NO,AOB,HAO}$	$K_{NH2OH,AOB}$ $K_{O2,AOB,2}$
NN pathway			$\eta_{AOB,NN}$			$\eta_{AOB,NN}$ $K_{NO,AOB,NN}$	
ND pathway				$\eta_{AOB,ND}$ $K_{O2,AOB,ND}$ $K_{I,O2,AOB,ND}$ $K_{HNO2,AOB}$		$\eta_{AOB,ND}$ $K_{I,O2,AOB,ND}$	$\eta_{AOB,ND}$ $K_{O2,AOB,ND}$ $K_{I,O2,AOB,ND}$ $K_{HNO2,AOB}$

Table 5. Parameters values of the 2-P model and specific kinetic rates (at 20°C, considering Arrhenius equation with θ_{AOB}=0.094 for growth rate).

Name	Description	Unit	Value	Source
μ_{AOB}	Maximum AOB growth rate	h^{-1}	0.0325	(Hiatt and Grady, 2008)
Y_{AOB}	AOB growth yield	$mgCODX.mgN^{-1}$	0.15	(Ni et al., 2013a)
$i_{N,BM}$	Nitrogen content of biomass	$mgN.mgCODX^{-1}$	0.07	(Henze, 2000)
$\eta_{AOB,ND}$	Reduction factor applied for the ND pathway	Dimensionless	0.250 ±0.011	Estimated
$\eta_{AOB,NN}$	Reduction factor applied for the NN pathway	Dimensionless	0.0015 ±0.001	Estimated
$K_{NH3,AOB}$	AOB affinity constant for NH_3	$mgN.L^{-1}$	0.20 ±0.08	Estimated
$K_{NH2OH,AOB}$	AOB affinity constant for NH_2OH	$mgN.L^{-1}$	0.90 ±0.11	Estimated
$K_{HNO2,AOB}$	AOB affinity constant for HNO_2	$mgN.L^{-1}$	0.004 ±0.003	Estimated
$K_{NO,AOB,HAO}$	AOB affinity constant for NO (from HAO)	$mgN.L^{-1}$	$3\ 10^{-4}$ $\pm 2.10^{-5}$	Estimated
$K_{NO,AOB,NN}$	AOB affinity constant for NO (from NirK)	$mgN.L^{-1}$	0.008 ±0.006	Estimated
$K_{I,O2,AOB}$	N_2O constant for production inhibition by O_2	$mgO_2.L^{-1}$	0.8 ±0.09	Estimated
$K_{O2,AOB,ND}$	AOB constant for O_2 effect on ND (rate 5)	$mgO_2.L^{-1}$	0.5 ±0.09	Estimated
$K_{O2,AOB,1}$	AOB affinity constant for O_2 (AMO reaction)	$mgO_2.L^{-1}$	1.0 ±0.14	Estimated
$K_{O2,AOB,2}$	AOB affinity constant for O_2 (HAO reaction)	$mgO_2.L^{-1}$	0.6 ±0.16	Estimated
$q_{AOB,AMO}$	Maximum rate for AMO reaction	$mgN.mgCODX^{-1}.h^{-1}$	0.2167	μ_{AOB}/Y_{AOB}
$q_{AOB,HAO}$	Maximum rate for HAO reaction	$mgN.mgCODX^{-1}.h^{-1}$	0.2167	μ_{AOB}/Y_{AOB}
$q_{AOB,N2O,ND}$	Maximum N_2O production rate by ND pathway	$mgN.mgCODX^{-1}.h^{-1}$	0.0542	$q_{AOB,HAO} \cdot \eta_{AOB,ND}$
$q_{AOB,N2O,NN}$	Maximum N_2O production rate by NN pathway	$mgN.mgCODX^{-1}.h^{-1}$	$3.25\ 10^{-4}$	$q_{AOB,HAO} \cdot \eta_{AOB,NN}$

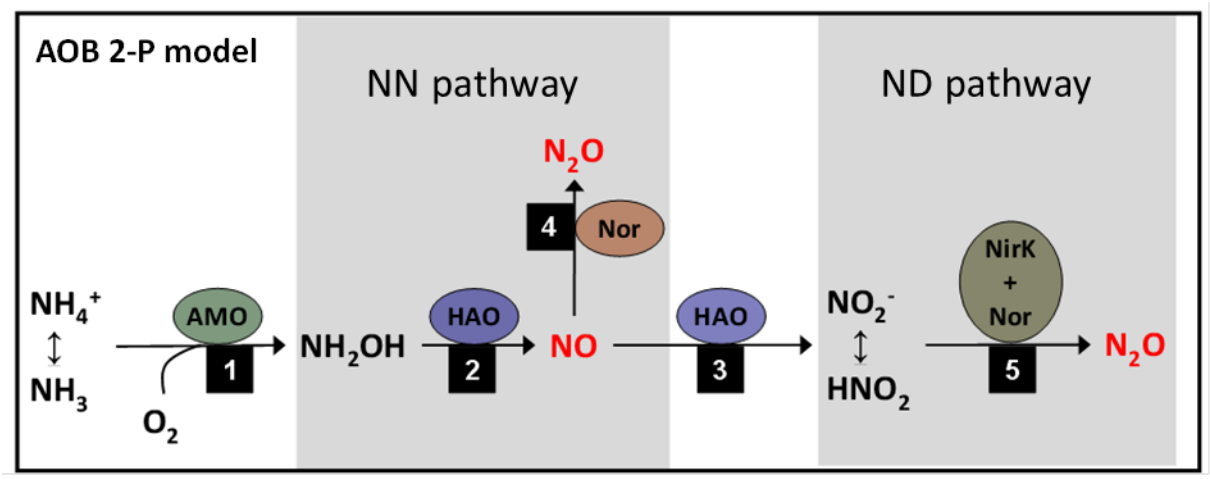

Figure 1. Schematic representation of the reactions involved in the two pathway model

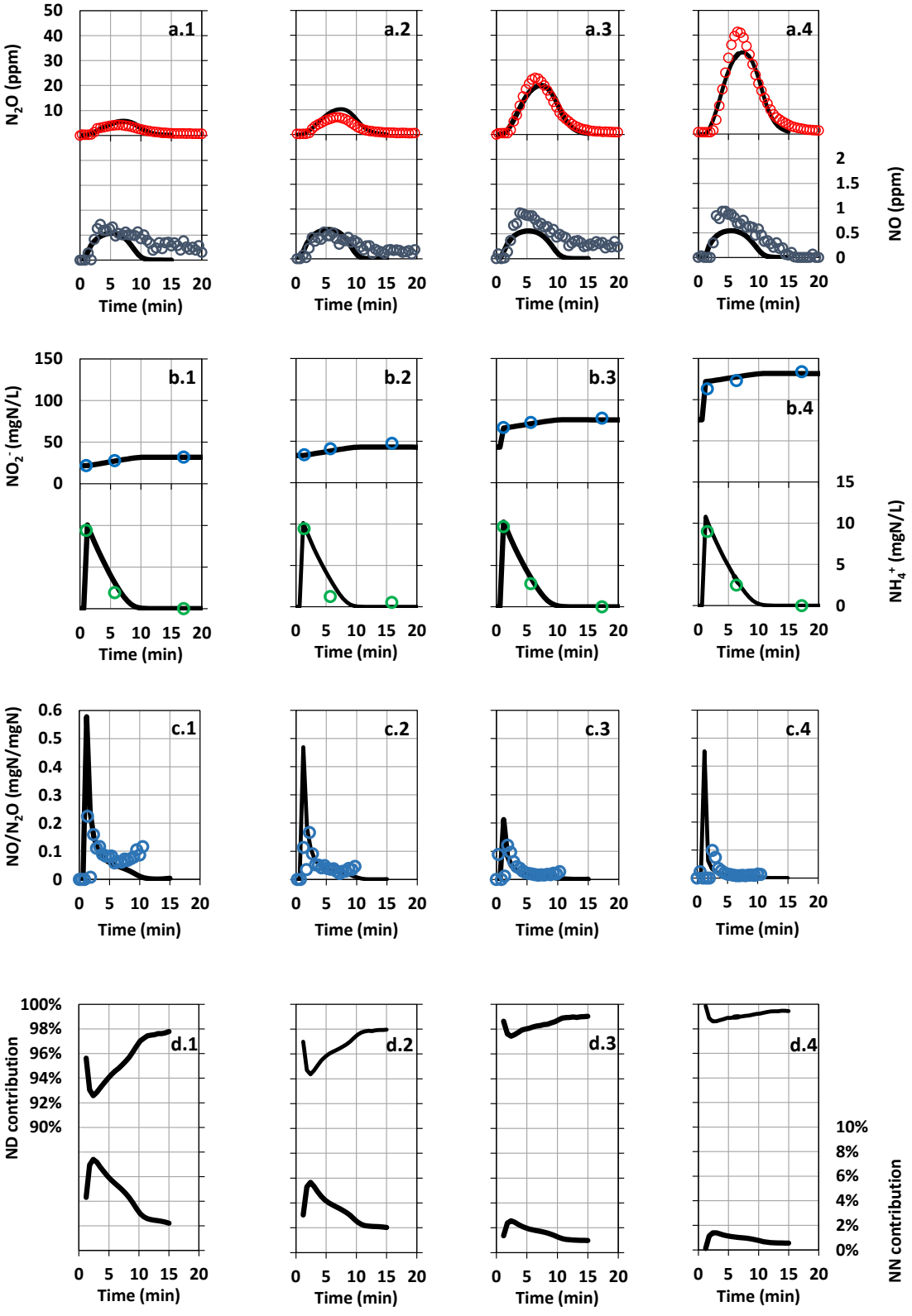

Figure 2. Experimental data (points) and simulation with the 2-P model (lines) for four aerobic batch tests with ammonia injections (10 mgN/L) and oxidation to nitrite for different initial nitrite concentrations. (a) NO and N_2O concentration in the gas phase (ppm); (b) Ammonia and nitrite concentrations; (c) NO/N_2O ratio; Simulated relative contributions of NN and ND pathways to N_2O emission (d).

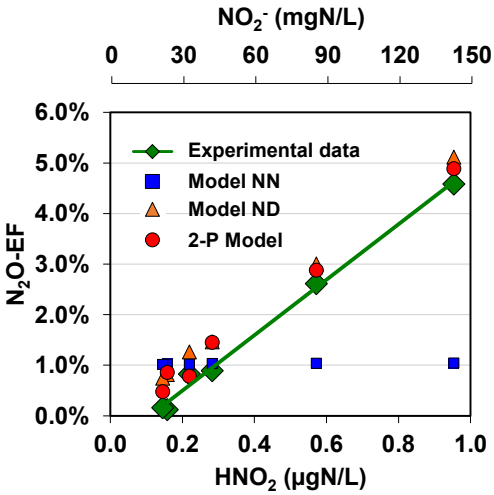

a

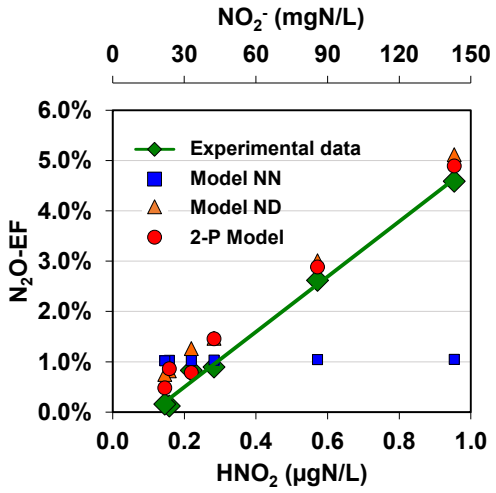

b

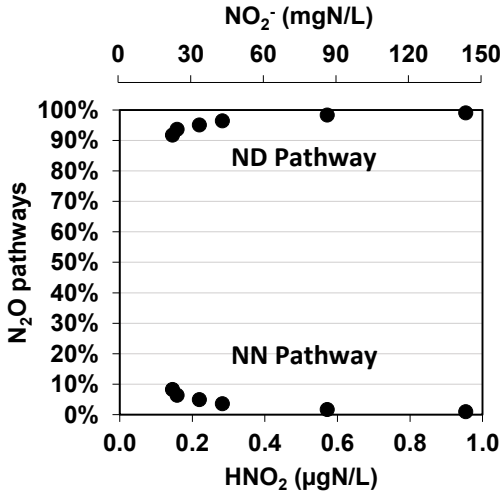

c

Figure 3. N_2O emission factor (EF) as a function of HNO_2 or nitrite concentration (a); NO-EF/N_2O-EF ratio as a function of HNO_2 or nitrite concentration (b); Simulated relative contributions of NN and ND pathways (c).

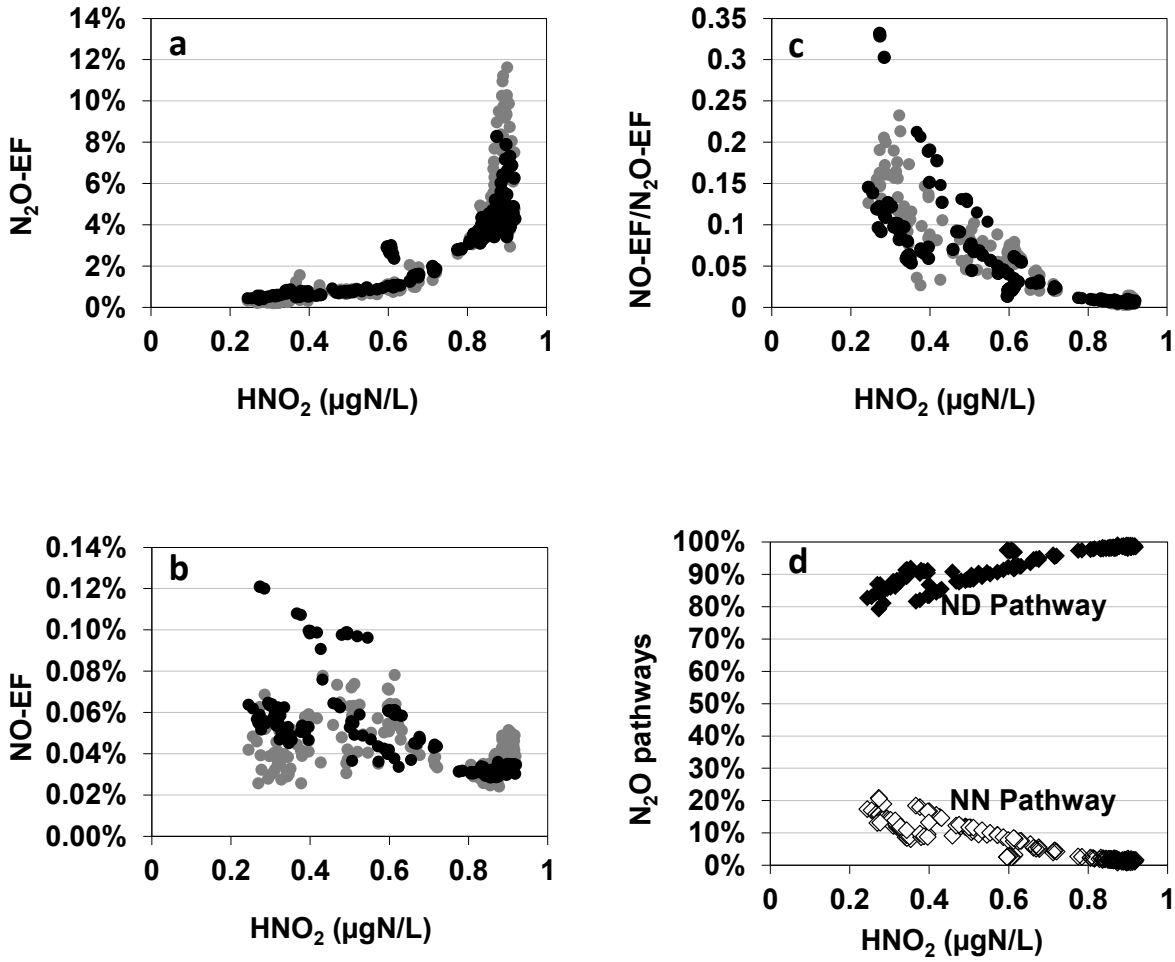

Figure 4. Simulated results (black) and experimental data (grey) for 187 cycles of the SBR (One dot = one cycle). N_2O (a), NO (b), the NO-EF/N_2O-EF ratio (c), versus the HNO_2 concentration. Simulated relative contributions of NN and ND pathways (d).

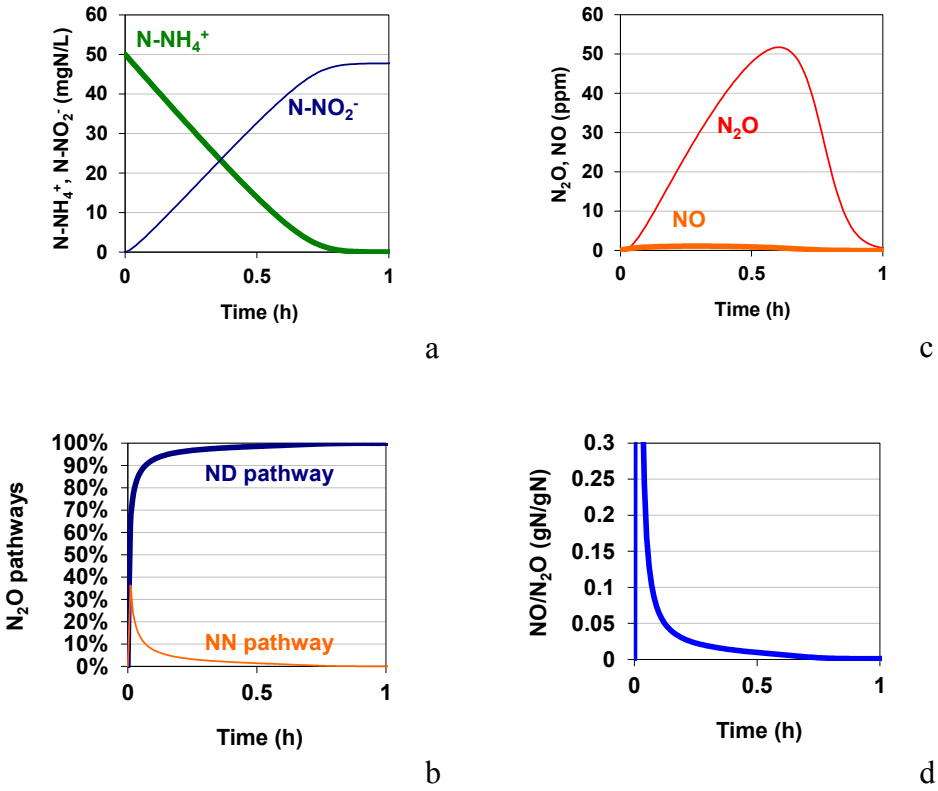

Figure 5. Simulated NO, N_2O, NO/N_2O ratio and contributions from the ND and NN pathways during a batch experiment.

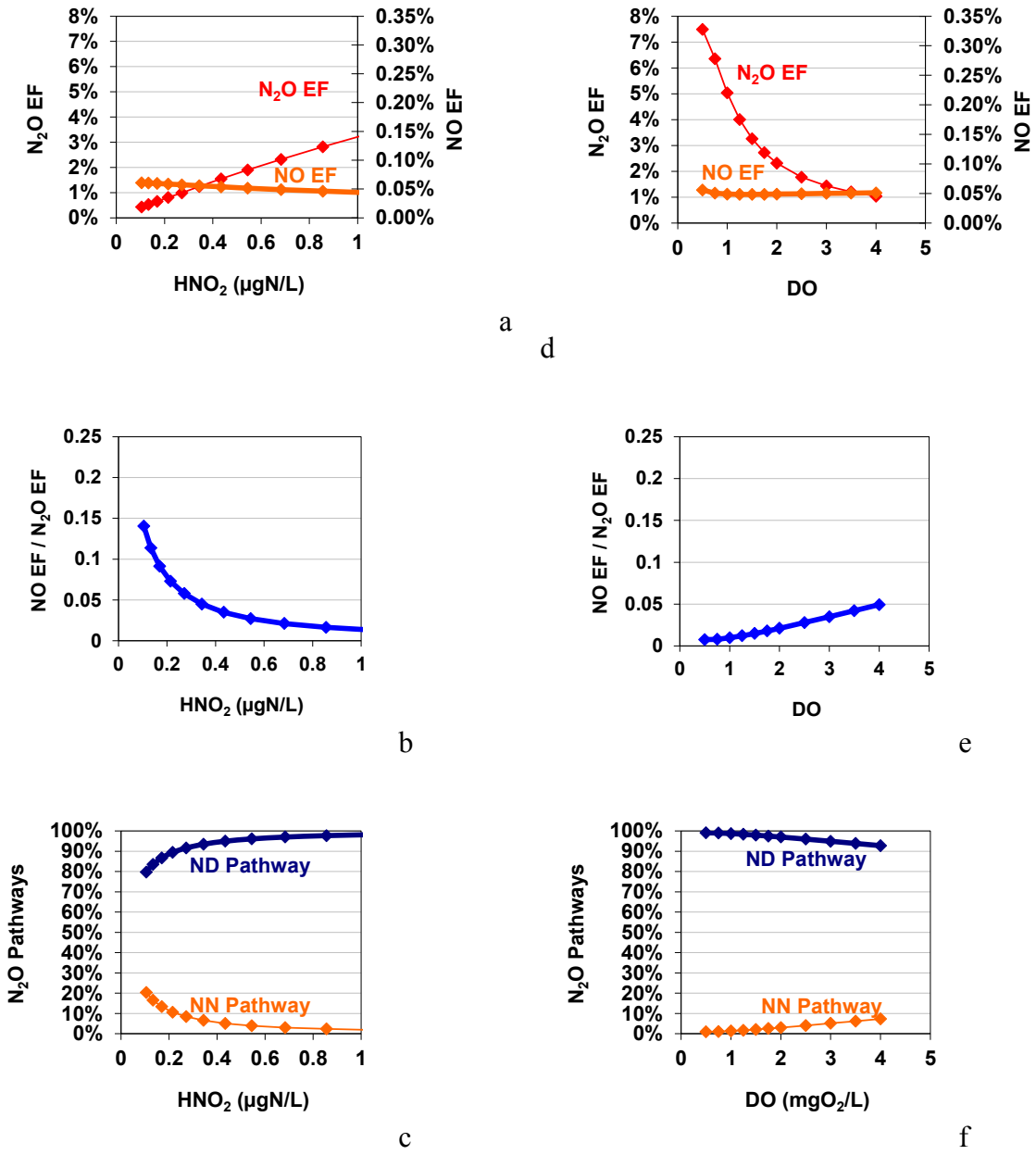

Figure 6. Simulations obtained for different HNO_2 and DO concentrations. The HNO_2 range was explored at a constant DO (2 $mgO_2.L^{-1}$) and, similarly, the range of DO was explored at a constant HNO_2 concentration (0.7 µgN-$HNO_2.L^{-1}$)